Density of States and Spectral Function of a Superconductor out of a Quantum-Critical Metal

Shang-Shun Zhang and Andrey V. Chubukov
School of Physics and Astronomy and William I. Fine Theoretical Physics Institute, University of Minnesota, Minneapolis, Minnesota 55455, USA

(Received 30 January 2023; accepted 25 July 2023; published 22 August 2023)

We analyze the validity of a quasiparticle description of a superconducting state above a metallic quantum-critical point (QCP). A normal state at a QCP is a non-Fermi liquid with no coherent quasiparticles. A superconducting order gaps out low-energy excitations, except for a sliver of states for non-s-wave gap symmetry, and at a first glance, restores coherent quasiparticle behavior. We argue that this does not necessarily hold as the fermionic self-energy may remain singular above the gap edge. This singularity gives rise to markedly non-BCS behavior of the density of states and to the appearance of a nondispersing mode at the gap edge in the spectral function. We analyze the set of quantum-critical models with an effective dynamical four-fermion interaction $V(\Omega) \propto 1/\Omega^{\gamma}$, where Ω is a frequency of a boson, which mediates the interaction. We show that coherent quasiparticle behavior in a superconducting state holds for $\gamma < 1/2$, but breaks down for larger γ. We discuss signatures of quasiparticle breakdown and compare our results with the photoemission data for Bi2201 and Bi2212.

DOI: 10.1103/PhysRevLett.131.086502

Introduction.—Metals near a quantum-critical point (QCP) display a number of non-Fermi-liquid properties like linear-in-T resistivity, a broad peak in the spectral function near k_F with linear-in-ω width, singular behavior of optical conductivity, etc. [1–19]. These properties are often associated with the coupling between fermions and near-gapless fluctuations of an order parameter, which condenses at a QCP [20–30].

The same fermion-boson interaction gives rise to a dome of superconductivity around a QCP [31–43]. A superconducting order gaps out low-energy excitations, leaving, at most, a tiny subset of gapless states for a non-s-wave order parameter, and a general belief has been that this restores fermionic coherence. A frequently cited experimental evidence is the observed emergence of a quasiparticle peak below T_c in near-optimally doped cuprates (see, e.g., Ref. [44]). From the theory side, it has been shown that fermionic self-energy in a superconductor above a QCP has a conventional Fermi-liquid form at the lowest ω, even when the gap has nodes [45], in distinction from a non-Fermi-liquid self-energy in the normal state [46–55].

In this Letter, we challenge the narrative that fermions in a superconducting state above a QCP are coherent quasiparticles. We argue that for a set of models, specified below, with an effective boson-mediated dynamical interaction $V(\Omega) \propto 1/|\Omega|^{\gamma}$, the fermionic self-energy deep in a superconducting state is singular on the real frequency axis above the gap edge at $\omega = \Delta$. This singularity gives rise to markedly non-BCS behavior of the density of states (DOS) and to broadening and eventual vanishing of the dispersing quasiparticle peak in the spectral function $A(\boldsymbol{k}, \omega)$, which gets replaced by a dispersionless mode, confined to the gap edge.

To put our results into perspective, it is instructive to compare them with superconductivity away from a QCP, mediated by a massive boson. There, $A(\boldsymbol{k}, \omega)$ at $T = 0$ displays a dispersing δ-functional peak at $|\omega| = (\Delta^2 + \xi_{\boldsymbol{k}}^2)^{1/2}$, where $\xi_{\boldsymbol{k}} = v_F(k - k_F)$ is a fermionic dispersion. This holds up to $|\omega| < \Delta + \omega_0$, where ω_0 is the mass of a pairing boson. At larger ω, fermionic damping kicks in, and the peak broadens. This results in peak-dip-hump behavior of $A(\boldsymbol{k}, \omega)$, observed most spectacularly in near-optimally doped cuprate $Bi_2Sr_2CaCu_2O_{8+\delta}$ (see, e.g., Refs. [56,57]). At a QCP, ω_0 vanishes and damping is present at all $\omega > \Delta$. The issue, which we address here, is whether the quasiparticle description survives, i.e., the width of the dispersing peak remains smaller than its energy, or quasiparticle description breaks down. We argue that the answer depends on the value of the exponent γ in the effective interaction. For $\gamma < 1/2$, the quasiparticle description survives, for $\gamma > 1/2$, it breaks down. In the last case, the DOS displays a power-law behavior with a non-BCS exponent and the spectral function displays a dispersionless mode confined to the gap edge. The dispersing quasiparticle peak survives for $\gamma \geq 1/2$ but eventually washes out, first for $\xi_{\boldsymbol{k}} > 0$ and then for $\xi_{\boldsymbol{k}} < 0$. We illustrate this in Fig. 1. We argue that our theory provides compelling interpretation of the angle-resolved photoemission spectroscopy (ARPES) data for Bi2201 and Bi2212 [58,59].

Model.—For our study, we consider dispersionful fermions, Yukawa coupled to a massless collective boson.

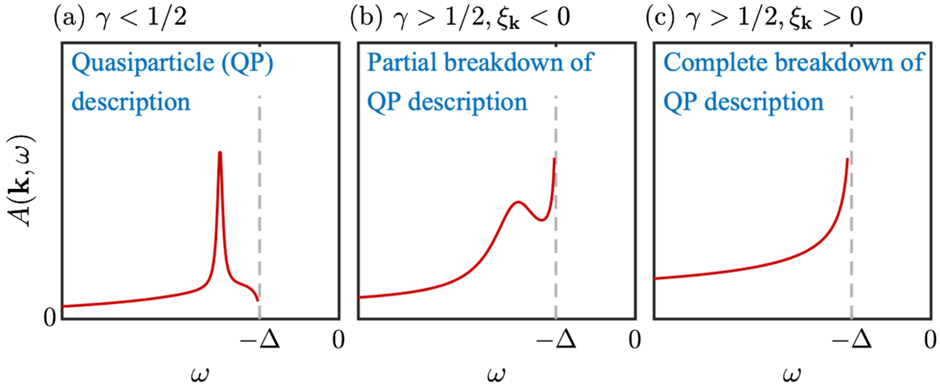

FIG. 1. Electronic spectral function $A(\boldsymbol{k}, \omega)$ at $T = 0$ in a quantum-critical superconductor at a finite $\xi_{\boldsymbol{k}} = v_F(k - k_F)$ for (a) the exponent $\gamma < 1/2$, (b) $\gamma \geq 1/2$, $\xi_{\boldsymbol{k}} < 0$, and (c) $\gamma \geq 1/2$, $\xi_{\boldsymbol{k}} > 0$. In (a), $A(\boldsymbol{k}, \omega)$ vanishes at $|\omega| = \Delta$ and has a well-defined dispersing peak at $\omega > \Delta$; i.e., fermions are coherent quasiparticles. In (b), quasiparticle peak broadens and a nondispersing mode appears at the gap edge. In (c), $A(\boldsymbol{k}, \omega)$ diverges at $|\omega| = \Delta$ and monotonically decreases at larger ω; i.e., a quasiparticle description completely breaks down.

In the normal state, a boson is Landau overdamped and is a slow mode compared to an electron in the sense that its effective velocity is far smaller than v_F [60]. In a superconductor, Landau damping is eliminated at frequencies below 2Δ as a feedback from pairing, yet bosons remain slow compared to electrons as long as $\Delta/k_F \ll v_F$. In this situation, the momentum integrations transverse and along the Fermi surface in the expressions for the normal and anomalous self-energies at any loop order are factorized: the one transverse to the Fermi surface involves fast electrons, the one along the Fermi surface involves slower bosons. The latter yields an effective "local" dynamical interaction $V(\Omega)$ (an analog of $\alpha^2 F(\Omega)$ for the electron-phonon case). At a QCP, $V(\Omega)$ is singular at vanishing Ω in spatial dimension $D \leq 3$ and behaves as $V(\Omega) \propto (\bar{g}/\Omega)^\gamma$, where $\bar{g}$ is the effective fermion-boson coupling, and the exponent γ is determined by the underlying microscopic model (deep in the superconducting state $\gamma = 2/3$ for fermions near an Ising-nematic or Ising-ferromagnetic QCP and $\gamma = 1$ near a spin-charge density-wave QCP) [61]. We consider γ as a parameter and aim at finding universal features, which hold for these and other models. We keep $\gamma \leq 1$ to avoid interference with the phase slips of the gap function on the real axis, which emerge at $\gamma > 1$ (Refs. [62,63]). We note that the same effective interaction $V(\Omega)$ emerges for dispersionless fermions in a quantum dot, coupled to Einstein bosons [the Yukawa-Sachdev-Ye-Kitaev (Yukawa-SYK) model] [64–67]. In this last case, the exponent γ is a continuous variable $\gamma \in (0, 1)$, depending on the ratio of fermion and boson flavors [68]. For simplicity, we neglect extra features associated with non-s-wave pairing symmetry and focus on $A(\boldsymbol{k}, \omega)$ away from the nodal points and on features in the DOS near the gap edge.

Pairing gap and quasiparticle residue.—For superconductivity mediated by a dynamical interaction, the pairing gap on a real frequency axis is complex, $\Delta(\omega) = \Delta'(\omega) + i\Delta''(\omega)$, and is a function of the running fermionic frequency ω. We define the gap edge Δ from the condition $\Delta(\omega) = \Delta'(\omega) = \Delta$ at $\omega = \Delta - 0$. We measure the deviation from the gap edge in $\delta = (\omega - \Delta)/\Delta$ and introduce $D(\omega) = \Delta(\omega)/\omega$. In a BCS superconductor (the case $\gamma = 0$ in our notations), $D(\omega) - 1 \approx -\delta$.

For a finite γ, the gap equation without vertex corrections has the same form as in the Eliashberg theory for electron-phonon interaction, but with $V(\Omega)$ instead of a phonon $\alpha^2 F(\Omega)$. Vertex corrections from higher-loop diagrams are generally of order one [69]. We assume that they do not affect the physics qualitatively and neglect them [70]. For justification, we note that the value of a superconducting T_c, obtained within the Eliashberg theory, near an antiferromagnetic QCP, agrees quite well with quantum Monte Carlo result [80].

The gap equation on the real frequency axis has been obtained before [62,81]. For any γ, $\Delta \sim \bar{g}$. We present the equation for arbitrary ω in the Supplemental Material [70] and here focus on $\omega = \Delta(1 + \delta)$ near the gap edge. For these ω, the gap equation simplifies to

$$D[\Delta(1 + \delta)] = 1 - a\delta + C(\delta), \tag{1}$$

where $a = O(1)$, $C(\delta) = C[\Delta(1 + \delta)] - C(\Delta)$, and

$$C(\omega) \sim \bar{g}^{\gamma - 1} \sin\frac{\pi\gamma}{2} \int_0^\omega \frac{d\Omega}{\Omega^\gamma} \frac{D(\omega - \Omega) - D(\omega)}{\sqrt{D^2(\omega - \Omega) - 1}}. \tag{2}$$

Whether the BCS-like description is valid now depends on whether or not $C(\delta) \ll \delta$. Assuming that this is the case and solving (1) iteratively, we obtain $C(\delta) \sim \delta^{3/2-\gamma}$. The assumption is then valid at $\gamma < 1/2$. Evaluating $C(\delta)$ explicitly, we obtain slightly above the gap edge, at $\delta > 0$,

$$\begin{aligned} D'[\Delta(1 + \delta)] &= 1 - a\delta + b\cos[\pi(3/2 - \gamma)]\delta^{3/2-\gamma}, \\ D''[\Delta(1 + \delta)] &= -b\sin[\pi(3/2 - \gamma)]\delta^{3/2-\gamma}, \end{aligned} \tag{3}$$

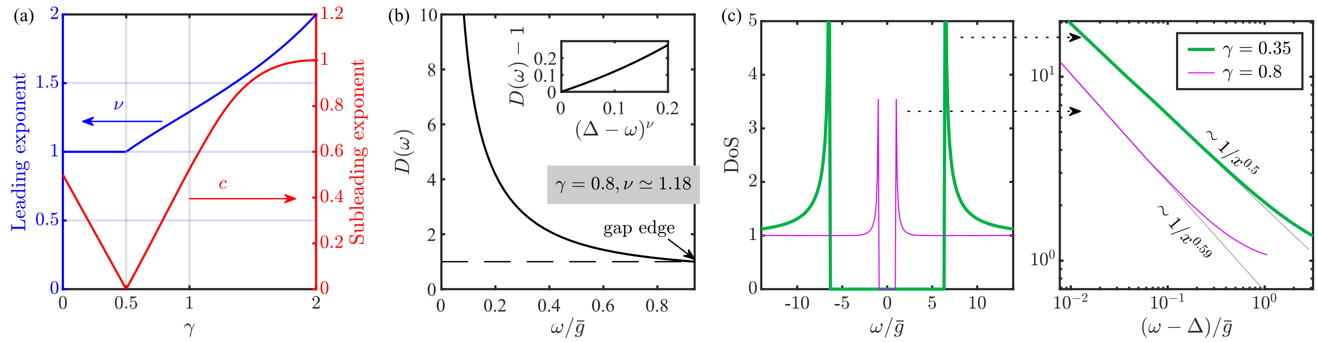

FIG. 2. (a) Exponents ν and c for the leading and the subleading terms in the expansion $D(\omega) \simeq 1 + a(\Delta-\omega)^\nu + b(\Delta-\omega)^{\nu+c}$, where $D(\omega) = \Delta(\omega)/\omega$ and the gap edge Δ is the solution of $D(\omega=\Delta)=1$. (b) Numerical result for $D(\omega)$ for $\gamma=0.8$. Inset: power-law behavior near the gap edge with $\nu=1.18$, consistent with (a). (c) Fermionic DOS at $T=0$ for $\gamma=0.35$ (thick green line) and $\gamma=0.8$ (thin pink line). In both cases, the DOS vanishes below the gap edge Δ and has a power-law singularity above it $N(\omega)\propto 1/(\omega-\Delta)^{\nu/2}$, but the exponent ν is different in the two cases, as we show in the right panel.

where $b\sim\sqrt{a}\sin(\pi\gamma/2)J(\gamma,1)$ and $J(\gamma,\nu)$ is expressed via Beta functions as

$$J(\gamma,\nu) = B\left(1-\gamma,\gamma-1-\frac{\nu}{2}\right) - B\left(1-\gamma,\gamma-1+\frac{\nu}{2}\right). \quad (4)$$

The function $D[\Delta(1+\delta)]$ is nonanalytic for $\gamma>0$, but still $D'-1 \gg D''$, and the leading term in $D-1$ is the regular one $-a\delta$. For $\gamma>1/2$, the calculation of $D[\Delta(1+\delta)]$ has to be done differently. We find after straightforward analysis that the leading term in $D[\Delta(1+\delta)]$ is nonanalytic and of order δ^ν, where $\nu>1$ is the solution of $J(\gamma,\nu)=0$. The exponent $\nu\approx 1+0.67(\gamma-1/2)$ for $\gamma\approx1/2$. The subleading term in $D[\Delta(1+\delta)]$ scales as $\delta^{\nu+c}$, where $c>0$ is approximately linear in $\gamma-1/2$. In Fig. 2, we plot $\nu(\gamma)$ and $c(\gamma)$ along with the numerical results of $D(\omega)$ for a representative $\gamma=0.8$. The exponent ν, extracted from the numerical $D(\omega)$, is 1.18, which matches perfectly with the analytical result. The behavior at $\gamma=1/2$ is somewhat special, see the Supplemental Material [70].

Another relevant quantity is the inverse fermionic residue $Z(\omega)=1+\Sigma(\omega)/\omega$, where $\Sigma(\omega)$ is the electronic self-energy. Near the gap edge, $Z[\Delta(1+\delta)] = Z+\bar{C}(\delta)$, where $Z=Z(\Delta)$, $\bar{C}(\delta)=\bar{C}[\Delta(1+\delta)]-\bar{C}(\Delta)$, and

$$\bar{C}(\omega)\sim\frac{\bar{g}^\gamma\sin\frac{\pi\gamma}{2}}{\omega}\int_0^\omega\frac{d\Omega}{\Omega^\gamma}\frac{1}{\sqrt{D^2(\omega-\Omega)-1}}. \quad (5)$$

This function is readily obtained once $D(\omega)$ is known. For $\gamma<1/2$, $Z[\Delta(1+\delta)]=Z+O(\delta^{1/2-\gamma})$ is approximately a constant near the gap edge. For $\gamma>1/2$, it is singular and scales as $1/\delta^{\nu/2+\gamma-1}$, where $\nu/2+\gamma-1>0$. In explicit form,

$$Z'[\Delta(1+\delta)] = \bar{b}\cos[\pi(\gamma+\nu/2-1)]\delta^{1-\gamma-\nu/2}, \quad (6)$$

$$Z''[\Delta(1+\delta)] = \bar{b}\sin[\pi(\gamma+\nu/2-1)]\delta^{1-\gamma-\nu/2}, \quad (7)$$

where $\bar{b}\sim\sin(\pi\gamma/2)/\sqrt{a}B[1-\gamma,(\nu/2)+\gamma-1]$.

Spectral function and DOS.—The spectral function and the DOS per unit volume are given by

$$A(\boldsymbol{k},\omega) = -\frac{1}{\pi}\mathrm{Im}G_R(\boldsymbol{k},\omega), \quad (8)$$

$$N(\omega) = \frac{1}{V}\sum_{\boldsymbol{k}}A(\boldsymbol{k},\omega) = N_F\mathrm{Im}\sqrt{\frac{1}{D^2(\omega)-1}}, \quad (9)$$

where the retarded Green's function $G_R(\boldsymbol{k},\omega) = -[\omega Z(\omega)+\xi_{\boldsymbol{k}}]/\{\xi_{\boldsymbol{k}}^2+[\omega Z(\omega)]^2[D^2(\omega)-1]\}$, and $\xi_{\boldsymbol{k}} = v_F(k-k_F)$ is the fermionic dispersion. ARPES intensity is proportional to $A(\boldsymbol{k},\omega)n_F(\omega)$, which at $T=0$ selects negative ω. At $\gamma=0$ (the BCS limit), $N[\Delta(1+\delta)]\sim 1/\delta^{1/2}$, and the spectral function has a δ-functional peak at the dispersing $\omega=(\Delta^2+\xi_{\boldsymbol{k}}^2)^{1/2}\approx\Delta+\xi_{\boldsymbol{k}}^2/(2\Delta)$. For a finite $\gamma<1/2$, these results hold, according to our calculations. The spectral function broadens, but still for any nonzero $\xi_{\boldsymbol{k}}$, $A(\boldsymbol{k},\Delta)=0$. The quasiparticle peak at a finite $\xi_{\boldsymbol{k}}$ is well defined, as its width $O(\xi_{\boldsymbol{k}}^{3-2\gamma})$ is parametrically smaller than its frequency. On the Fermi surface, at $\xi_{\boldsymbol{k}}=0$, $A(\boldsymbol{k},\Delta(1+\delta))\sim\mathrm{Im}1/(\delta+i\delta^{3/2-\gamma})$. The integral of $A(\boldsymbol{k}_F,\omega)$ over an infinitesimally small range around $\delta=0$ is finite, as it is expected for an integral around a quasiparticle peak.

For $\gamma>1/2$, system behavior changes. Now $N[\Delta(1+\delta)]\propto1/\delta^{\nu/2}$ diverges near $\omega=\Delta$ with a different, γ-dependent exponent, and $A(\xi_{\boldsymbol{k}},-\Delta(1+\delta))$ diverges at the gap edge for any $\xi_{\boldsymbol{k}}$. At a finite $\xi_{\boldsymbol{k}}$ it diverges as $A(\boldsymbol{k},\Delta(1+\delta))\propto1/\delta^{\nu/2+\gamma-1}$, and at $\xi_{\boldsymbol{k}}=0$ as $A(\boldsymbol{k}_F,\Delta(1+\delta))\propto1/\delta^{\nu/2+1-\gamma}$. In the last case, the integral of $A(\boldsymbol{k}_F,\Delta(1+\delta))$ over an infinitesimally small range of δ vanishes, which can be interpreted as the disappearance of a quasiparticle peak at $\xi_{\boldsymbol{k}}\to0$.

In Figs. 2(c) and 2(d), we show $N(\omega)$, obtained from the numerical solution of the full gap equation [70] for representative $\gamma=0.35$ and 0.8. We see that in both cases

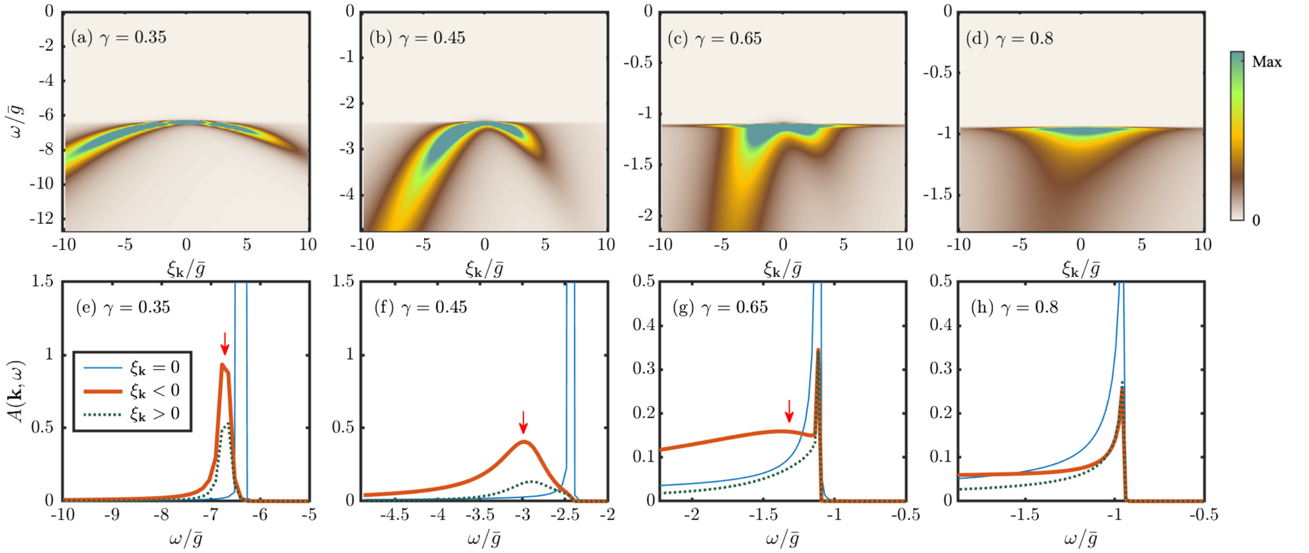

FIG. 3. Spectral function $A(\boldsymbol{k},\omega)$ at $T = 0$ for four representative γ. The broadening in the plots is intrinsic. (a)–(d) Color-coded plot at negative ω, as measured by the ARPES intensity at T = 0. (e)–(h) Constant-$\boldsymbol{k}$ cuts of $A(\boldsymbol{k},\omega)$ at $\xi_{\boldsymbol{k}} = 0$ and at $\xi_{\boldsymbol{k}} = \pm 4\bar{g}$. For $\gamma < 1/2$, the spectral function has a sharp quasiparticle peak at $\omega + \Delta \propto \xi_{\boldsymbol{k}}^2$. For $\gamma > 1/2$, the peak moves to $\omega + \Delta \propto |\xi_{\boldsymbol{k}}|^{1/(1-\gamma)}$ and broadens up, which eventually disappears (see text).

the DOS is a gapped continuum, but the behavior near the gap edge is qualitatively different: for $\gamma = 0.35$, $N(\omega)$ has the same $1/\delta^{1/2}$ singularity as for $\gamma = 0$, and for $\gamma = 0.8$, the DOS behaves as $\delta^{-\nu/2}$, where $\nu \simeq 1.18$. The numerical results for the spectral function $A(\boldsymbol{k},\omega)$ are shown in Fig. 3 for several γ. For comparison with ARPES, we set ω to be negative. For any γ, the spectral function is nonzero for all $|\omega| > \Delta$ simply because the bosonic mass vanishes at a QCP. Still, for $\gamma < 1/2$ [Figs. 3(a) and 3(b)], the numerical results show a well-defined dispersing quasiparticle peak, whose width is smaller than its energy for both positive and negative $\xi_{\boldsymbol{k}}$. This is the same behavior as in Fig. 1(a).

For $\gamma > 1/2$ [Figs. 3(a) and 3(b)], we see that $A(\xi_{\boldsymbol{k}},\omega)$ becomes singular at the gap edge for any $\xi_{\boldsymbol{k}}$. For $\gamma < 0.9$, the frequency dependence of $A(\boldsymbol{k},\omega)$ is monotonic for $\xi_{\boldsymbol{k}} > 0$ and nonmonotonic for $\xi_{\boldsymbol{k}} < 0$. For the latter, the spectral function has a kink at the gap edge $\omega = -\Delta$ and a hump at $\omega = -\Delta - O(|\xi_{\boldsymbol{k}}|^{1/(1-\gamma)})$. This is the same behavior as in Figs. 1(b) and 1(c). For larger γ, $A(\boldsymbol{k},\omega)$ monotonically decreases away from gap edge for both positive and negative $\xi_{\boldsymbol{k}}$.

Comparison with ARPES.—The behavior shown in Fig. 4 and illustrated in Figs. 1(b) and 1(c) is consistent with the ARPES data for Bi2201, Ref. [58]. The data shows that the spectral function near the antinode, where our analysis is valid, displays an almost nondispersing maximum at positive $\xi_{\boldsymbol{k}}$ (i.e., outside the Fermi surface), while for negative $\xi_{\boldsymbol{k}}$ it displays a nondispersing kink at the same energy as for positive $\xi_{\boldsymbol{k}}$ and a dispersing maximum (a hump) at larger $|\omega|$. We associate the nondispersing feature at both positive and negative $\xi_{\boldsymbol{k}}$ with the singularity at the gap edge and associate the dispersing hump at $\xi_{\boldsymbol{k}} < 0$ with the one in Figs. 4(a) and 1(b). A very similar behavior, with gap-edge singularity and a broad peak at higher frequencies, has been observed in Bi2212 [59] (see also [82,83]).

With respect to the origin of a soft boson, our results are consistent with antiferromagnetic spin fluctuations, for which deep in the superconducting state, $\gamma = 1$ at energies below the gap, where spin fluctuations are propagating, and $\gamma = 1/2$ at larger energies, where they become Landau overdamped. At intermediate $\omega, \Omega \sim \Delta$, the exponent γ interpolates between $1/2$ and 1. This is what we need for the behavior in Fig. 4. More generally, our results are consistent with either spin or charge QCP toward an order

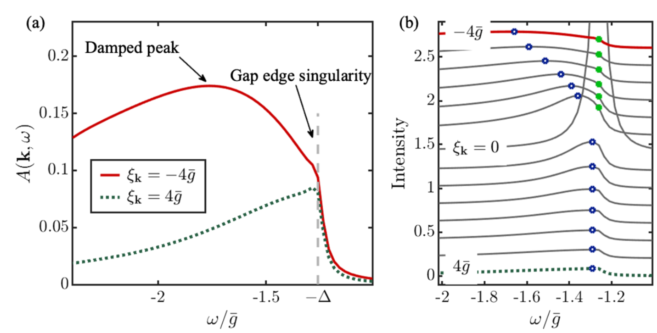

FIG. 4. (a) Spectral function $A(\boldsymbol{k},\omega)$ at $\gamma = 0.6$ for positive and negative $\xi_{\boldsymbol{k}} = \pm 4\bar{g}$. To account for impurity scattering, we convoluted the spectral function with a Lorentzian of width $\sim 0.03\bar{g}$. (b) Spectral function at a discrete a set of momenta. It displays a nondispersing mode at the gap edge (green dots) for both positive and negative $\xi_{\boldsymbol{k}}$ and a dispersing hump, which exists only for negative $\xi_{\boldsymbol{k}}$ (blue circles). This theoretical $A(\boldsymbol{k},\omega)$ is consistent with the ARPES data for Bi2201, Ref. [58] (see text).

with a finite momentum. They are less consistent with a $Q = 0$ QCP (e.g., a nematic one) as in this case the exponent γ interpolates between $2/3$ at smaller energies and $1/3$ at higher energies, such that at intermediate energies γ is either smaller than $1/2$ or too close to it. Also, a generalization of our analysis to other materials exhibiting quantum criticality, like heavy-fermion and iron-based superconductors, requires extra care and has to be done separately.

Discussion and summary.—In this Letter, we analyzed the applicability of a quasiparticle description deep inside a superconductor that emerges out of a non-Fermi liquid at a metallic QCP. We considered the model with an effective dynamical four-fermion interaction $V(\Omega) \propto 1/\Omega^\gamma$, mediated by a gapless boson at a QCP, and analyzed the spectral function and the DOS for $\gamma \in (0, 1)$. This interaction gives rise to a non-Fermi liquid in the normal state with the self-energy $\Sigma(\omega) \propto \omega^{1-\gamma}$ and to a pairing below some finite T_c. A superconducting order gaps out low-energy excitations and, at a first glance, should restore fermionic coherence. We found, however, that this holds only for $\gamma < 1/2$. For larger γ, the behavior of the spectral function and the DOS is qualitatively different from that in a superconductor with coherent quasiparticles. We found a different power-law behavior of the DOS above the gap edge, the emergence of a dispersionless mode confined to the gap edge, and the broadening and eventual disappearance of the dispersing quasiparticle peak.

Away from a QCP, a pairing boson is massive, and at the lowest energies a Fermi-liquid description holds already in the normal state and continues to hold in a superconductor. In the immediate vicinity of the gap edge, the system then displays a BCS-like behavior for all values of γ. Still, the behavior over a wider frequency range is governed by the physics at a QCP, as numerous experiments on the cuprates and other correlated systems indicate. We argued that our results are quite consistent with the ARPES data for Bi2201 and Bi2212 [11,58,59].

We acknowledge with thanks useful conversations with a number of our colleagues. This work was supported by the U.S.-Israel Binational Science Foundation (BSF). The work by A. V. C. was supported by U.S. Department of Energy, Office of Science, Basic Energy Sciences, under Award No. DE-SC0014402.

[1] S. Martin, A. T. Fiory, R. M. Fleming, L. F. Schneemeyer, and J. V. Waszczak, Phys. Rev. B **41**, 846 (1990).
[2] H. v. Löhneysen, T. Pietrus, G. Portisch, H. G. Schlager, A. Schröder, M. Sieck, and T. Trappmann, Phys. Rev. Lett. **72**, 3262 (1994).
[3] M. R. Norman, H. Ding, M. Randeria, J. C. Campuzano, T. Yokoya, T. Takeuchi, T. Takahashi, T. Mochiku, K. Kadowaki, P. Guptasarma *et al.*, Nature (London) **392**, 157 (1998).
[4] Z.-X. Shen and G. Sawatzky, Phys. Status Solidi (b) **215**, 523 (1999).
[5] S. Grigera, R. Perry, A. Schofield, M. Chiao, S. Julian, G. Lonzarich, S. Ikeda, Y. Maeno, A. Millis, and A. Mackenzie, Science **294**, 329 (2001).
[6] A. Damascelli, Z. Hussain, and Z.-X. Shen, Rev. Mod. Phys. **75**, 473 (2003).
[7] D. S. Inosov, J. Fink, A. A. Kordyuk, S. V. Borisenko, V. B. Zabolotnyy, R. Schuster, M. Knupfer, B. Büchner, R. Follath, H. A. Dürr, W. Eberhardt, V. Hinkov, B. Keimer, and H. Berger, Phys. Rev. Lett. **99**, 237002 (2007).
[8] R. Daou, N. Doiron-Leyraud, D. LeBoeuf, S. Li, F. Laliberté, O. Cyr-Choiniere, Y. Jo, L. Balicas, J.-Q. Yan, J.-S. Zhou *et al.*, Nat. Phys. **5**, 31 (2009).
[9] R. Cooper, Y. Wang, B. Vignolle, O. Lipscombe, S. Hayden, Y. Tanabe, T. Adachi, Y. Koike, M. Nohara, H. Takagi *et al.*, Science **323**, 603 (2009).
[10] T. Sarkar, P. R. Mandal, J. S. Higgins, Y. Zhao, H. Yu, K. Jin, and R. L. Greene, Phys. Rev. B **96**, 155449 (2017); K. Jin, N. Butch, K. Kirshenbaum, J. Paglione, and R. Greene, Nature (London) **476**, 73 (2011).
[11] M. Hashimoto, I. M. Vishik, R.-H. He, T. P. Devereaux, and Z.-X. Shen, Nat. Phys. **10**, 483 (2014).
[12] A. Kaminski, T. Kondo, T. Takeuchi, and G. Gu, Philos. Mag. **95**, 453 (2015).
[13] B. Keimer, S. A. Kivelson, M. R. Norman, S. Uchida, and J. Zaanen, Nature (London) **518**, 179 (2015).
[14] L. Taillefer, Annu. Rev. Condens. Matter Phys. **1**, 51 (2010).
[15] A. Legros, S. Benhabib, W. Tabis, F. Laliberté, M. Dion, M. Lizaire, B. Vignolle, D. Vignolles, H. Raffy, Z. Li *et al.*, Nat. Phys. **15**, 142 (2019).
[16] C. M. Varma, Rev. Mod. Phys. **92**, 031001 (2020).
[17] S. A. Hartnoll and A. P. Mackenzie, Rev. Mod. Phys. **94**, 041002 (2022).
[18] K. Harada, Y. Teramoto, T. Usui, K. Itaka, T. Fujii, T. Noji, H. Taniguchi, M. Matsukawa, H. Ishikawa, K. Kindo, D. S. Dessau, and T. Watanabe, Phys. Rev. B **105**, 085131 (2022).
[19] S. Sur and S.-S. Lee, Phys. Rev. B **90**, 045121 (2014); **91**, 125136 (2015); **94**, 195135 (2016).
[20] H. v. Löhneysen, A. Rosch, M. Vojta, and P. Wölfle, Rev. Mod. Phys. **79**, 1015 (2007).
[21] T. Valla, A. Fedorov, P. Johnson, B. Wells, S. Hulbert, Q. Li, G. Gu, and N. Koshizuka, Science **285**, 2110 (1999).
[22] A. Abanov, A. V. Chubukov, and J. Schmalian, Adv. Phys. **52**, 119 (2003); J. Electron Spectrosc. Relat. Phenom. **117**, 129 (2001).
[23] J. Fink, A. Koitzsch, J. Geck, V. Zabolotnyy, M. Knupfer, B. Büchner, A. Chubukov, and H. Berger, Phys. Rev. B **74**, 165102 (2006).
[24] T. Shibauchi, A. Carrington, and Y. Matsuda, Annu. Rev. Condens. Matter Phys. **5**, 113 (2014).
[25] F. Restrepo, U. Chatterjee, G. Gu, H. Xu, D. K. Morr, and J. C. Campuzano, Commun. Phys. **5**, 45 (2022).
[26] D. J. Scalapino, Rev. Mod. Phys. **84**, 1383 (2012).
[27] K. B. Efetov, H. Meier, and C. Pepin, Nat. Phys. **9**, 442 (2013).
[28] S. Lederer, Y. Schattner, E. Berg, and S. A. Kivelson, Proc. Natl. Acad. Sci. U.S.A. **114**, 4905 (2017).
[29] S. A. Hartnoll, D. M. Hofman, M. A. Metlitski, and S. Sachdev, Phys. Rev. B **84**, 125115 (2011).

[30] H. Wang and G. Torroba, Phys. Rev. B **96**, 144508 (2017).
[31] N. E. Bonesteel, I. A. McDonald, and C. Nayak, Phys. Rev. Lett. **77**, 3009 (1996).
[32] A. Abanov, A. V. Chubukov, and A. M. Finkel'stein, Europhys. Lett. **54**, 488 (2001).
[33] A. V. Chubukov, A. Abanov, Y. Wang, and Y.-M. Wu, Ann. Phys. (Amsterdam) **417**, 168142 (2020).
[34] M. A. Metlitski, D. F. Mross, S. Sachdev, and T. Senthil, Phys. Rev. B **91**, 115111 (2015).
[35] A. Perali, C. Castellani, C. Di Castro, and M. Grilli, Phys. Rev. B **54**, 16216 (1996).
[36] E. G. Moon and S. Sachdev, Phys. Rev. B **80**, 035117 (2009).
[37] Y. Wang and A. V. Chubukov, Phys. Rev. Lett. **110**, 127001 (2013).
[38] Y. Wang, A. Abanov, B. L. Altshuler, E. A. Yuzbashyan, and A. V. Chubukov, Phys. Rev. Lett. **117**, 157001 (2016).
[39] H. Wang, S. Raghu, and G. Torroba, Phys. Rev. B **95**, 165137 (2017).
[40] D. T. Son, Phys. Rev. D **59**, 094019 (1999); A. V. Chubukov and J. Schmalian, Phys. Rev. B **72**, 174520 (2005).
[41] A. Abanov and A. V. Chubukov, Phys. Rev. B **102**, 024524 (2020).
[42] E. A. Yuzbashyan, Michael K.-H. Kiessling, and B. L. Altshuler, Phys. Rev. B **106**, 064502 (2022).
[43] S.-S. Zhang, Y.-M. Wu, A. Abanov, and A. V. Chubukov, Phys. Rev. B **106**, 144513 (2022).
[44] A. Kaminski, J. Mesot, H. Fretwell, J. C. Campuzano, M. R. Norman, M. Randeria, H. Ding, T. Sato, T. Takahashi, T. Mochiku, K. Kadowaki, and H. Hoechst, Phys. Rev. Lett. **84**, 1788 (2000).
[45] D. J. Scalapino, Rev. Mod. Phys. **84**, 1383 (2012).
[46] V. Oganesyan, S. A. Kivelson, and E. Fradkin, Phys. Rev. B **64**, 195109 (2001).
[47] W. Metzner, D. Rohe, and S. Andergassen, Phys. Rev. Lett. **91**, 066402 (2003); L. Dell'Anna and W. Metzner, Phys. Rev. B **73**, 045127 (2006).
[48] J. Rech, C. Pépin, and A. V. Chubukov, Phys. Rev. B **74**, 195126 (2006).
[49] M. A. Metlitski and S. Sachdev, Phys. Rev. B **82**, 075127 (2010); **82**, 075128 (2010).
[50] D. F. Mross, J. McGreevy, H. Liu, and T. Senthil, Phys. Rev. B **82**, 045121 (2010).
[51] S. Raghu, G. Torroba, and H. Wang, Phys. Rev. B **92**, 205104 (2015); A. L. Fitzpatrick, S. Kachru, J. Kaplan, S. Raghu, G. Torroba, and H. Wang, Phys. Rev. B **92**, 045118 (2015).
[52] A. Klein, A. V. Chubukov, Y. Schattner, and E. Berg, Phys. Rev. X **10**, 031053 (2020).
[53] S.-S. Lee, Phys. Rev. B **80**, 165102 (2009); D. Dalidovich and S.-S. Lee, Phys. Rev. B **88**, 245106 (2013); A. Schlief, P. Lunts, and S.-S. Lee, Phys. Rev. X **7**, 021010 (2017).
[54] M. Punk, Phys. Rev. B **94**, 195113 (2016).
[55] D. L. Maslov and A. V. Chubukov, Phys. Rev. B **81**, 045110 (2010).
[56] D. S. Dessau, B. O. Wells, Z.-X. Shen, W. E. Spicer, A. J. Arko, R. S. List, D. B. Mitzi, and A. Kapitulnik, Phys. Rev. Lett. **66**, 2160 (1991).
[57] A. A. Kordyuk, S. V. Borisenko, T. K. Kim, K. A. Nenkov, M. Knupfer, J. Fink, M. S. Golden, H. Berger, and R. Follath, Phys. Rev. Lett. **89**, 077003 (2002).
[58] R.-H. He, M. Hashimoto, H. Karapetyan, J. Koralek, J. Hinton, J. Testaud, V. Nathan, Y. Yoshida, H. Yao, K. Tanaka *et al.*, Science **331**, 1579 (2011).
[59] W.-S. Lee, I. Vishik, K. Tanaka, D. Lu, T. Sasagawa, N. Nagaosa, T. Devereaux, Z. Hussain, and Z.-X. Shen, Nature (London) **450**, 81 (2007).
[60] As an example, for an instability with momentum $q = 0$, the bosonic propagator is $\chi(q,\Omega) = 1/(q^2 - i\gamma\Omega/q)$, and the dispersion relation for a collective mode is $\Omega \sim q^3/\gamma$. At small enough q, the effective bosonic velocity $v_b \sim q^2/\gamma$ is parametrically smaller than v_F. Typical q^2 is obtained by analyzing relevant scales for the self-energy and is of order $v_F\gamma(\bar{g}/E_F)$. The effective bosonic velocity $v_b \sim v_F(\bar{g}/E_F)$ is smaller than v_F when the Yukawa coupling $\bar{g}$ is small compared to the Fermi energy (see, e.g., Ref. [84]).
[61] In the normal state, the corresponding exponents are $1/3$ near an Ising-nematic or Ising-ferromagnetic QCP and $1/2$ near a spin-charge density-wave QCP.
[62] Y.-M. Wu, S.-S. Zhang, A. Abanov, and A. V. Chubukov, Phys. Rev. B **103**, 024522 (2021).
[63] Y.-M. Wu, S.-S. Zhang, A. Abanov, and A. V. Chubukov, Phys. Rev. B **103**, 184508 (2021).
[64] I. Esterlis and J. Schmalian, Phys. Rev. B **100**, 115132 (2019); D. Hauck, M. J. Klug, I. Esterlis, and J. Schmalian, Ann. Phys. (Amsterdam) **417**, 168120 (2020).
[65] Y. Wang, Phys. Rev. Lett. **124**, 017002 (2020).
[66] D. Chowdhury and E. Berg, Phys. Rev. Res. **2**, 013301 (2020).
[67] L. Classen and A. Chubukov, Phys. Rev. B **104**, 125120 (2021).
[68] An extension of the Yukawa-SYK model to $\gamma \in (1,2)$ has recently been proposed [85].
[69] J. Rech, C. Pépin, and A. V. Chubukov, Phys. Rev. B **74**, 195126 (2006).
[70] See Supplemental Material at http://link.aps.org/supplemental/10.1103/PhysRevLett.131.086502 for the derivation of the gap equation in real frequencies and its numerical solution, the analysis of the special case of $\gamma = 1/2$, the derivation of the universal form of the spectral function for $1/2 < \gamma < 1$, and the analysis of the validity of the Eliashberg theory, which includes Refs. [52,71–79].
[71] Y.-M. Wu, A. Abanov, Y. Wang, and A. V. Chubukov, Phys. Rev. B **102**, 024525 (2020).
[72] F. Marsiglio and J. P. Carbotte, Phys. Rev. B **43**, 5355 (1991); for more recent results see F. Marsiglio and J. P. Carbotte, in *The Physics of Conventional and Unconventional Superconductors*, edited by Bennemann and Ketterson (Springer-Verlag, Berlin, 2006) and references therein; F. Marsiglio, Ann. Phys. (Amsterdam) **417**, 168102 (2020).
[73] A. Karakozov, E. Maksimov, and A. Mikhailovsky, Solid State Commun. **79**, 329 (1991).
[74] R. Combescot, Phys. Rev. B **51**, 11625 (1995).
[75] Y.-M. Wu, A. Abanov, Y. Wang, and A. V. Chubukov, Phys. Rev. B **99**, 144512 (2019).

[76] A. V. Chubukov, A. Abanov, I. Esterlis, and S. A. Kivelson, Ann. Phys. (Amsterdam) **417**, 168190 (2020).
[77] J. Rech, C. Pépin, and A. V. Chubukov, Phys. Rev. B **74**, 195126 (2006).
[78] B. L. Altshuler, L. B. Ioffe, and A. J. Millis, Phys. Rev. B **50**, 14048 (1994).
[79] S.-S. Lee, Annu. Rev. Condens. Matter Phys. **9**, 227 (2018).
[80] X. Wang, Y. Schattner, E. Berg, and R. M. Fernandes, Phys. Rev. B **95**, 174520 (2017).
[81] F. Marsiglio, M. Schossmann, and J. P. Carbotte, Phys. Rev. B **37**, 4965 (1988).
[82] A. A. Kordyuk, S. V. Borisenko, T. K. Kim, K. A. Nenkov, M. Knupfer, J. Fink, M. S. Golden, H. Berger, and R. Follath, Phys. Rev. Lett. **89**, 077003 (2002).
[83] A. Damascelli, Z. Hussain, and Z.-X. Shen, Rev. Mod. Phys. **75**, 473 (2003).
[84] S.-S. Zhang, E. Berg, and A. V. Chubukov, Phys. Rev. B **107**, 144507 (2023).
[85] J. Schmalian (private communication).